Research on Engineering Structures & Materials
www.jresm.org
Research Group

Research Article

Experimental investigation of reinforced concrete corbels with different concrete strengths and shear span-to-depth ratios under monotonic loading

Ahmed Y. A. Zainul-Abideen [1,a], Muhammad Abed Attiya [1,b], Ola Mazen Makki [*,2,c]

[1]*Dept. of Civil Engineering, Faculty of Engineering, University of Kufa, Al-Najaf, Iraq*
[2]*Dept. of Civil Engineering, College of Engineering, University of Al-Qadisiyah, Al-Qadisiyah, Iraq*

Article Info

Article History:

Received 29 May 2026

Accepted 12 Aug 2026

Keywords:

Concrete capacity;
Crack patterns of corbels;
Corbel ultimate load;
Collapse mechanism of corbels

Abstract

Corbels are structural connections between beams and columns that provide support to slabs and, in some cases, act as short cantilever beams. A compression strut is typically formed within the corbel, where failure often initiates. Since this strut functions as a short-concealed column, its strength primarily depends on the compressive strength of the concrete and the a/d ratio. This study aims to investigate the influence of different concrete compressive strengths on the behavior and ultimate load capacity of corbels, as well as the influence of geometry on corbel resistance. Eight specimens were cast and tested to examine these parameters. Four models with varying mixes were investigated, and the gained concrete compressive strengths (15, 20, 25, and 30 MPa) were considered, while the other four specimens investigated the influence of varying the a/d ratio as (1, 0.75, 0.5, and 0.35). The results indicated that the ultimate load increased by 11.5%, 37%, and 85% for specimens with compressive strengths of 20, 25, and 30 MPa, respectively, compared to the specimen with 15 MPa. Additionally, the concrete strength had a significant impact on the initial cracking load (or appearance of the first crack), indicating a direct relationship between corbel performance and material strength. Additionally, the corbel strength rises when a/d is minimized. In terms of deflection at failure, specimens with higher a/d ratios showed larger deflections, whereas specimens with lower a/d ratios displayed stiffer behavior and smaller deflections at failure.

1. Introduction

Corbels are cantilevers with very short spans monolithic with (or fixed to) columns to provide support for slabs (or precast beams or girders) for resting on them as shown in Fig.1. Due to their short projection, corbels typically have a shear span-to-depth ratio (a/d) of less than 1.0. Consequently, load is transferred primarily via a strut-and-tie mechanism similar to deep beams, requiring structural engineers to design them against shear-dominated failure modes [1–6].

The main failure modes for members lacking stirrups include shear failure, flexural tensile strength, crushing of the concrete of the strut, and diagonal splitting. The previously mentioned failure modes typically fall under the title of one concept, which is a beam-shear failure. This mode is distinguished by forming one or more diagonal shear cracks, which are subsequently merged to form complete shear failure at the strut zone [3, 7–9].

Brackets and corbels are short-haunched cantilevers that extend from the inner face of columns or concrete walls to support heavy concentrated loads from precast beams, gantry girders, and other precast systems. Typically, the shear arm to depth ratio is less than 1.0, leading to nonlinear stress

*Corresponding author: Ola.Mazen@qu.edu.iq
[a]orcid.org/0009-0005-1754-1684; [b]orcid.org/0000-0001-8914-0875; [c]orcid.org/0009-0008-0839-0716
DOI: http://dx.doi.org/10.17515/resm2026-1717ma0529rs

behavior influenced by shear deformation within the elastic range. As a result, the shear strength of the section becomes a crucial design consideration. Special attention should be given to the design of corbels, as the strength of a precast concrete structure largely depends on the compression capacity of its connections instead of the individual members' strengths. Considering that the corbel is a key component in connecting a beam and a column, it must be designed as a stronger member than the beam and column together [10–14].

Fig. 1. Some types of corbels in buildings [15, 16]

Different sizes and reinforcement of corbel specimens (a total of 22 modes) were investigated to discuss their shear behavior during monotonic loads by Huang Y. et al [5], and it was concluded that the additional stirrup reinforcement enhances the collapse load of corbels, increasing it by 15% to 46% compared to corbels without stirrups. Also, developing the concrete compressive strength (f'c) significantly improves the safety level in the triangular truss model. In other words, when the compressive strength increases from 30 to 70 MPa, the safety margin increases from 1.28 to 1.87. In contrast, the strut-and-tie model shows an initial increase in safety level, followed by a decrease as the compressive strength improves. Specifically, when f'c is modified from 30 to 50 MPa, the safety margin rises from 1.07 to 1.32, but then decreases to 1.2 when the strength is further increased to 70 MPa.

An experimental investigation was made to study the effect of corbel concrete compressive strength and its behavior under shear stresses by Sayhood E. et al [17], and it was concluded that an increase in compressive strength from 23 to 48.6 MPa leads to the development of the nominal shear strength. Moreover, the increase in steel reinforcement ratio causes an increment in the corbel's nominal shear strength. This effect is not included in the ACI 318M-2019 [2] provisions, making the code proposal conservative. L.J. Mahmood and F.R Karim [19] reviewed the impact of fiber, concrete strength, reinforcement ratio, and shear span-to-depth ratio on the shear resistance of reinforced fibrous high-strength concrete corbels in earlier studies. The findings indicate that corbels' shear resistance increases when primary reinforcement, compressive strength, and fiber volume percentage rise, whereas it falls as the corbel's shear span-to-effective depth ratio rises. Furthermore, depending on the fiber specifications, adding fibers to high-strength reinforced concrete corbels enhances their ductility and, thus, determines their mode of failure. Lei H. et al [20] examine the shear failure and crack development of reinforced concrete corbels with and without web reinforcement using an experimental program that includes six large-scale experiments. The influence of predetermined inclined fractures at the corbel corner, the shear span-to-depth ratio, and the reinforcing inclination are the primary factors. Additionally included are the comprehensive test data for rotational deformations, shear strength, and fracture kinematics. Lastly, the physical function of the inclined reinforcement, the impact of corner fractures, the application constraints, and the suggested approach's future development are examined. To quickly analyze the shear strength of existing RC corbels during maintenance and strengthening, this method clearly explains the failure processes.

Traad H.Z et al [21] study looks at a way to improve reinforced concrete corbels using either post-tension cables or the pre-stressing tendons themselves, which are run through freshly bored cable conduits. The results of an experimental investigation of eight prestressed corbels with different shear span to depth ratios and pre-stressing tendon locations are presented. Strands with a diameter of 15.24 mm were used to post-tension the corbels. The results of the experiments were examined in relation to the load-bearing capacity and cracking behavior of short cantilevers reinforced with passive reinforcement, emphasizing the impact of the corbel's load capacity and the shear ratio, which is the most significant factor influencing cracking.

While prior research has examined the effects of concrete compressive strength and the shear span-to-effective depth ratio (a/d) separately, consistent experimental datasets that concurrently assess their impact on several structural performance indicators under identical testing conditions are still lacking in the literature. By offering a thorough experimental evaluation of reinforced concrete corbels, including ultimate load, load–deflection behavior, crack propagation, initial stiffness, ductility, and toughness, the current study enhances the current experimental database and makes comparisons more trustworthy.

2. Experimental Program and Methodology

A total of eight corbels were cast and investigated with specified dimensions as sketched in Fig.2 and Fig.3. Four corbel specimens were cast with different strengths to view the influence of concrete compressive and tensile strengths on the behavior. The higher concrete compressive strength specimen (C30) was selected to cast the other four corbels with varying span-to-depth ratio (a/d). The column supporting the two cantilevered corbels was 0.2 m for both sides in cross-section and 0.45m long. Another four specimens were cast to investigate the changes in a/d ratios as (1, 0.75, 0.5, and 0.35).

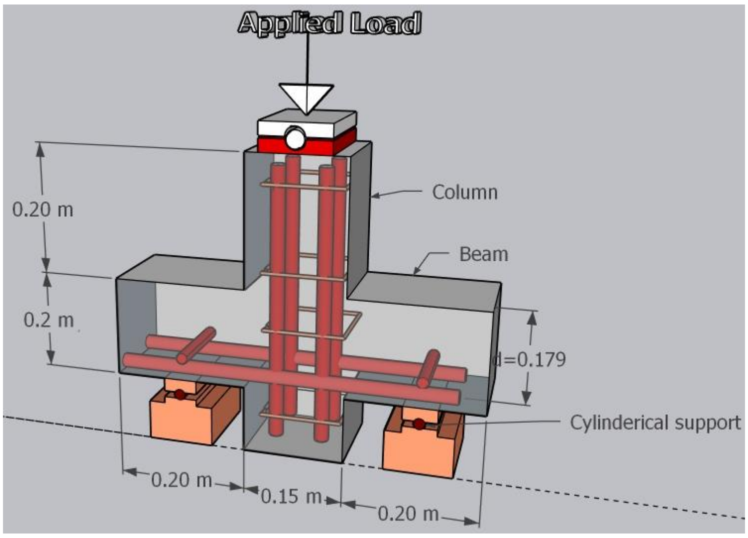

Fig. 2. Corbel dimensions and reinforcement details (all dimensions are in meters)

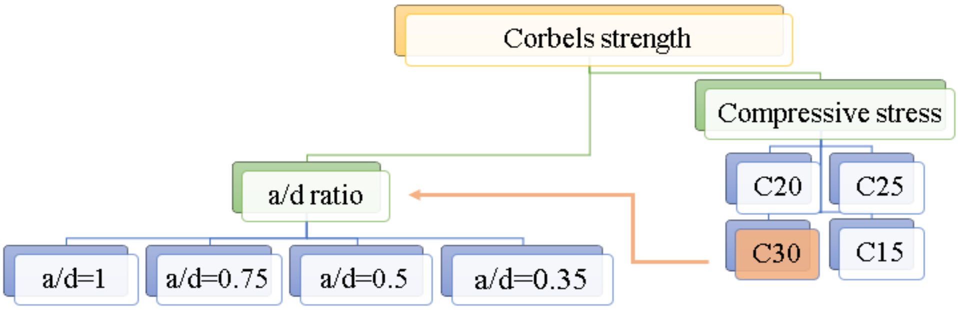

Fig. 3. Experimental program flow chart

The cantilever projection length was selected as 0.2 m and the thickness was 0.15m at both faces of the column and the free end. The longitudinal reinforcement consisted of four deformed bars with a diameter of 12.7 mm, while 6.0 mm diameter bars were used as stirrups. The details of the experimental work, specimens' dimensions, and reinforcement could be clarified from Table 1. The primary steel rebars, which are of 12.7mm diameter, were placed at the bottom of the beam with an effective side cover of 0.025m. Bending steel reinforcement was welded with a cross bar of the same size, which lies near the end of each model to provide additional anchorage [14].

Table 1. Specimens' details and parameters

Group (Main testing variable)	Specimen	(f'c)	a	d(mm)	a/d	stirrup diameter and spacing	Cover (mm)	Loading Location
Group One (*F'c*)	C15	15.7	125	179	0.69	Ø6@125	25	Axial load at the column center using square bearing plate
	C20	20.2	125	179	0.69	Ø6@125	25	
	C25	25.31	125	179	0.69	Ø6@125	25	
	C30	29.9	125	179	0.69	Ø6@125	25	
Group Two (Geometry)	a/d=1	29.9	179	179	1	Ø6@125	25	
	a/d=0.75	29.9	134	179	0.75	Ø6@125	25	
	a/d=0.5	29.9	90	179	0.5	Ø6@125	25	
	a/d=0.35	29.9	63	179	0.35	Ø6@125	25	

3. Materials, Mixing and Load Application

The construction materials used for casting the models were ordinary Portland cement, sand, gravel, and reinforcing steel in addition to water. The property of each material was described separately as explained in the following sections.

3.1. Cement

From Kufa Cement Factory, a Portland cement that matches the Iraqi standard specification was adopted to be used for casting the corbels' specimens [22].

3.2. Aggregate

Both fine and coarse aggregate were provided from the natural quarry of Najaf city/Iraq and their gradation was determined by sieve analysis before casting. The aggregates complied with the Iraqi standard specifications for construction materials [23]. Fig.4 and Fig.5 show the sieve analysis results of the sand sample, and it could be concluded that the fineness modulus of the sample equals 2.5 and the graduation similar to Zone 2.

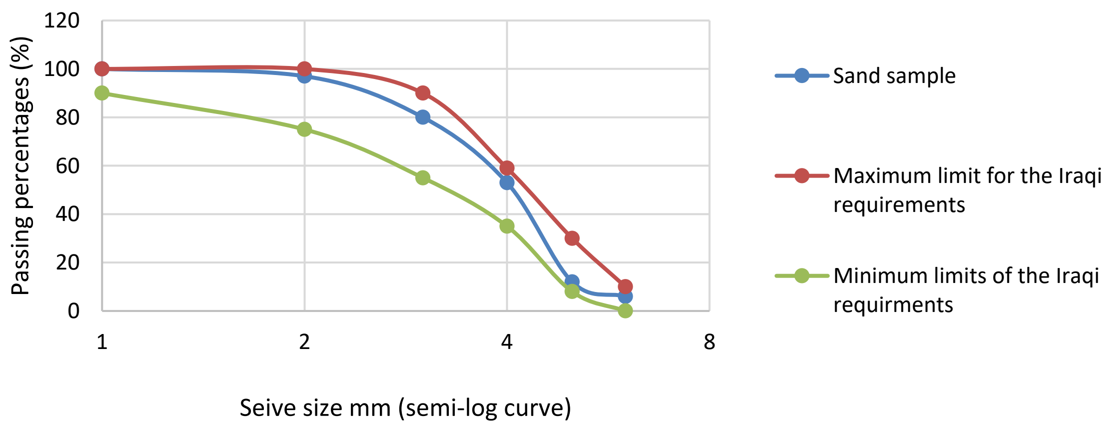

Fig. 4. Fine aggregate adopted sizes

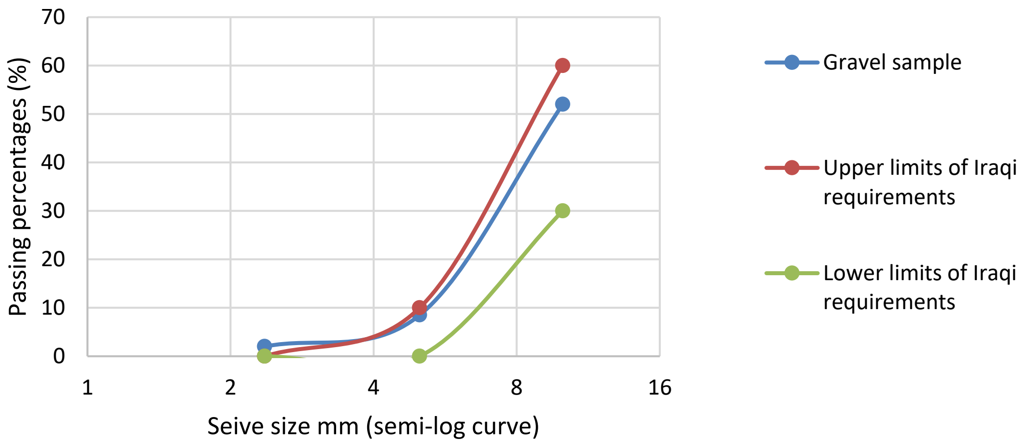

Fig. 5. Sieve analysis of coarse aggregates

3.3. Steel Reinforcing Bars

Ukrainian steel reinforcing bars were utilized as longitudinal reinforcement for the tested deep beams. Longitudinal steel bars for all tested corbels consisted of a bar diameter of 12.7mm while 6.0mm bars were used as lateral ties. The bars have been tested in the Material Laboratory of the Civil Engineering Department at Kufa University. The axial tensile test showed that the tested sample of Young's modulus equals 2*105 MPa, yielding stress of 560.2 MPa, and the rupture stress was 674.1 MPa.

3.4. Mixing of Concrete

Different concrete compressive strengths were adopted for casting four corbel specimens, and the variation in the strength was obtained from using different concrete mixes based on minimizing the gravel amount and maximizing the cement content. The utilized mixing proportions were 1:3:3, 1:2.7:2.7, 1:2.3:2.3, and 1:2:2, as explained in Table 2. After mixing the concrete as shown in Fig.6 and putting the corbel reinforcement within the molds at the correct spacing as shown in Fig. 7, the fresh concrete was cast, the surfaces were finished, and left to dry for one day, and then the molds were opened and the 28 days of curing started.

To test the concrete compressive strengths of all specimens, three cubes of each mix were cast for examining the strength after 28 days. Models after casting are illustrated in Fig.8. It is worth mentioning that the specimens were denoted by their compressive strength values, such as C15 for the corbel specimen, which f'c equals 15 MPa, etc. The strength of concrete was chosen to be structural and non-structural to investigate the effect of low strength on the overall structural behavior of corbels and to examine if its general behavior is influenced by the low strength or not, as well as considering that corbels are shear-critical deep members and behave similarly to deep beams [24]. The Specimens related to a/d ratios were denoted by (a/d=), then followed by the a/d number, such as a/d=0.5. All these four corbels were cast with concrete compressive strength equal to 30 MPa.

Table 2. Mix design

Mix proportion	Cement content (kg/m^3)	Sand (kg/m^3)	Gravel (kg/m^3)	Water (kg/m^3)	w/c	Max aggregate size (mm)	Theoretical Slump test (mm)	F_{cu} (MPa)	F'c (MPa)
1:3:3	310	1022	1150	235	0.76	10	42	22.4	15.7
1:2.7:2.7	344	927	1041	220	0.64	10	54	28.85	20.2
1:2.3:2.3	396	908	1024	205	0.52	10	71	36.15	25.31
1:2:2	461	921	979	193	0.42	10	82	42.71	29.9

Fig. 6. Preparation and mixing of concrete stages

Fig. 7. Steel reinforcement within the framework

Fig. 8. Corbel specimens and cubes after casting

3.5. Monotonic Load Application

A universal electrical control hydraulic press system was used for applying static load on the specimens with a maximum capacity of 2000 kN as applied load as shown in Fig.9. This portion compresses continuously during the testing process until the final failure load for the specimen. A dial gauge of 20 mm capacity was fixed on the specimen for tracking and recording the deflection at each load step. The corbel specimen under the applied load is illustrated in Fig.10.

Fig. 9. The universal testing machine

Fig. 10. Specimen within the pressing system during the monotonic test

A single specimen was investigated at the same time, with a load increment of 5 kN to closely monitor the appearance of the first crack. A square loading plate of 150 mm side length was used for all specimens to ensure good load distribution and avoid local failure. A dial gauge was installed beneath the model as shown in Fig.10. The supports used were hinge-to-roller supports.

One specimen was used to represent each test variable in this study, which is based on a small sample size. Therefore, rather than being statistically confirmed conclusions, the results should be considered as indicative experimental tendencies, and more testing is advised to validate the observed behavior.

3.6. Analytical Solution

Using a principal analysis for corbels using the strut-tie method [2, 24–26] for denoting the total capacity of specimens, the strength of corbels could be calculated as follows:

- $a = 125\ mm$
- $A_s = 253.4\ mm^2$
- $f_y = 560.2\ MPa$
- $d = 179$
- $T_n = A_s * f_y = 141.9\ kN$
- $V_{n\ for\ tie} = T_n * \left(\frac{d}{a}\right) = 203.279\ kN$
- $V_{n\ for\ strut} = 0.60\ bd\ \sqrt{f'c}$

After calculating the values of shear strength, Table 3 shows the results and the control capacities.

Table 3. Analysis of the corbels theoretically

Corbel	F'c (MPa)	a (mm)	d (mm)	$\boldsymbol{V_{n\ for\ strut}}$ $(\boldsymbol{kN})$	$\boldsymbol{V_{n\ for\ tie}}$ $(\boldsymbol{kN})$	Control capacity (kN)
C15	15.7	125	179	43.6	203.279	43.6
C20	20.2	125	179	50.3	203.279	50.3
C25	25.31	125	179	56.3	203.279	56.3
C30	29.9	125	179	61.6	203.279	61.6

4. Results and Discussions

4.1. Materials Results

4.1.1. Slump Test

As mentioned previously, four mixing proportions were used to discuss the concrete compressive strength, which were based on the gradual increment of cement ratio at the expense of the gravel quantity. The lower amount of cement and the higher magnitude of aggregate could be found at the 1:3:3 mix, in which the amount of binder coating the aggregate particles is less than required. The internal friction for such a mix rises, leading to reduced flowability; consequently, the measured slump was 38 mm. When slightly increasing the cement versus gravel content (1:2.7:2.7 mix), an enhancement in internal friction and workability could be gained; for that, the slump value develops to 54 mm, which is considered as low to moderate consistency. A significant enhancement in the paste volume of the mix when using the mixing proportion 1:2.3:2.3, which gained the mix more capability for coating the aggregate particles. Such improvement in lubrication influences minimizing the particle interlock and internal friction, so that the slump test at that mix equals 86mm, which is considered a moderately workable mix.

The mix that contains the minimum amount of aggregate and a higher percentage of cement compared to the previous mixes is 1:2:2. This mixing proportion showed the highest workability (93 mm) and the best particle interlocking due to the good lubrication and the sufficient binder coating the aggregates. When comparing the values of slump in Table 2 and the experimental workability test, it could be found differences in some millimeters due to the laboratory conditions, weather temperature, the limitations of theoretical calculations, aggregate absorption, cement fineness, and the amount of free water may differ.

4.1.2. Compressive Strength

It is expected logically to find a clear difference in concrete compressive strength for the four mixing proportions used in accordance with the sufficiency of cement within the mix or not. For the higher amounts of aggregate mixing, it is expected poor coating of the binder to the aggregate, due to the lower cement content. Therefore, earlier cracking was observed for such mixes, and that is what viewed at the mixing proportions 1:3:3 and 1:2.7:2.7. The concrete compressive strength of these mixes was 15.7 MPa and 20.2 MPa, respectively. These mixes contain a higher volume of capillary pores, and a large empty porous concrete matrix is comparatively weaker due to the limited hydration products, i.e., calcium silicate hydrate (C–S–H), which is the primary component responsible for strength in hardened concrete. It is worth mentioning that the first mix, C15, is considered non-structural concrete, but still needed to be investigated to view the corbel behavior with such amount of strength. After maximizing the amount of cement further by using mixing proportions 1:2.3:3 and 1:2:2, it could be noticed that the compressive strength jumped to 25.31 MPa and 29.9 MPa, respectively, which is due to an increase in the binder and producing more C–S–H gel.

4.2. Corbels Results

After testing the models under statically loading machine, the results of the 4 magnitudes of concrete corbel strengths are shown in Fig. 11, while the influence of changing the a/d ratio is illustrated in Fig. 12. From Table 4, the average experimental-to-predicted load ratio was 1.181, with a range of 1.053 to 1.428. The analytical approach produced cautious expectations for every tested corbel since all ratios were larger than unity.

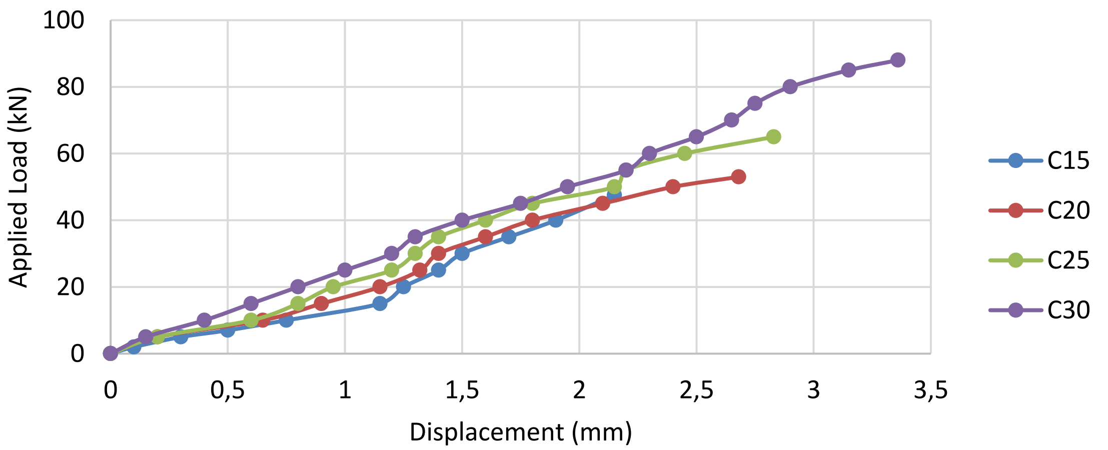

Fig. 11. Load versus displacement curves for all the tested specimens

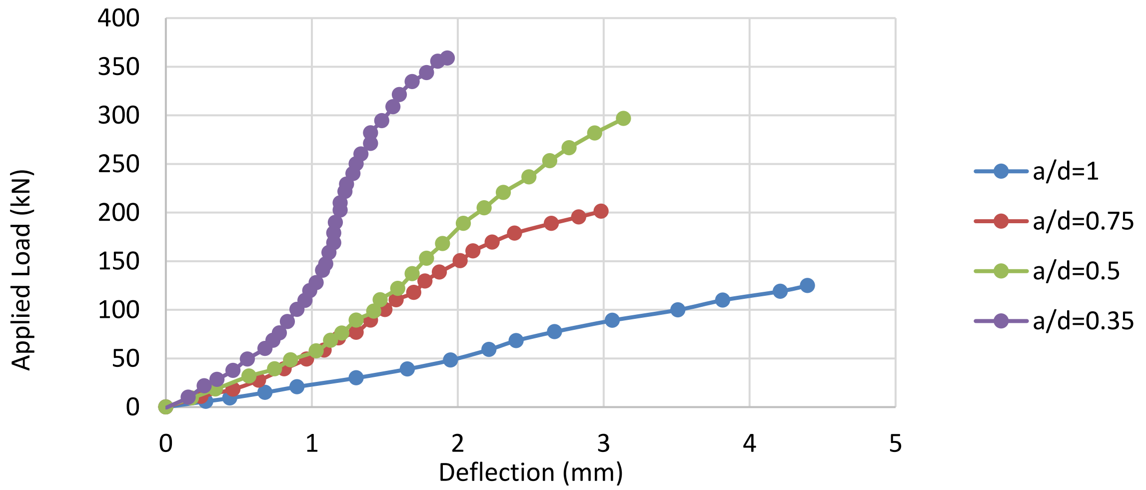

Fig. 12. Testing results of four corbels with different a/d ratios

The rather similar ratios found for specimens C15, C20, C25 and C30 show that the experimental and anticipated capabilities coincide fairly well. The analytical model's oversimplified assumptions and incomplete representation of resistance mechanisms, such as aggregate interlock, the longitudinal reinforcement's dowel action, improved bond and confinement, and the contribution of the welded transverse anchorage bar, may be the cause of this disparity. The efficiency of the nodal area and compression strut may have been enhanced by the increase in concrete strength. However, the observed variance should not be exclusively attributable to concrete strength because only one specimen was evaluated at each concrete-strength level.

Table 4. Comparison between theoretical predictions and ultimate experimental loads for the tested specimens

Corbel	Theoretical capacity	Experimental capacity	R
C15	43.6	47.5	1.089
C20	50.3	53	1.053
C25	56.3	65	1.154
C30	61.6	88	1.428

4.2.1. Load Versus Deflection Curves Discussions

Fig.11 introduces the load versus deflection curves for corbels of varying magnitudes of compressive strengths. It can be clearly seen that the models showed the same trends from the elastic stage to failure. The corbels behave elastically at first loading and show linear behavior until 30% of the collapse load; then the nonlinearity stage begins for all models. The plastic stage occurs for all models after observing an initial visible crack, after which the specimen could not return to its elastic deformation. When observing C15 and C20, they deflect close to each other and show similar deflection at each loading stage, but C15 collapses faster due to its weakness. Similarly, the same nearby curves for C25 and C30 tends but C25 was faster to be failed than C30. At the same magnitude of load (let’s take 40 kN), the displacement of the weaker corbels is less than that of the stronger. As a conclusion, corbels are generally affected by compressive strength by its failure load and maximum deflection significantly, but the compressive strength magnitude (even if it is non-structural (C15)) has no influence on curve behavior and general trends. Corbel's ultimate strength could be developed by 11.5%, 37%, and 85.8%, respectively, when enhancing compressive strength from C15 to C20, C25, and C30.

From observing Fig.12, which illustrates the impact of the a/d ratio on corbel behavior, it can be noticed that the trends of curve changes and the behavior were significantly affected by this ratio due to the strut formed, especially for model C15, while similar trends were observed for the structural concrete corbels. The linear behavior also ended after 30% of the failure load for all models, and the nonlinearity started after the first visible crack was seen on the specimen. Approximately the same trends were observed for the model’s a/d=0.5 and a/d=0.75 due to their approach values, but a huge difference was observed from the a/d=0.35 model due to the larger bottle-shaped strut forming.

Varying a/d from 1 to 0.75, 0.5, and 0.35, the overall ultimate corbel strength rises to 60.2%, 140.38%, and 187.4%, respectively, while the deflection decreases by 31.8%, 28.8%, and 56.3%. When observing the deflection at the same loading stage (let’s consider 100 kN), the model with a larger a/d ratio introduces higher deflection compared to the others, especially for the model with a/d=1.0. It deflects by 3.5 mm at 100 kN, while the other models are displaced by 1.46, 1.42, and 0.89 mm, respectively, at the same applied load. This is due to the high stiffness and the effect of deep beams showed clearly at high a/d ratio corbels, making the failure always at strut collapse and with no influence of flexure, so that the deflection of the a/d=0.35 specimen was the minimum among the others because it compressed, failed by strut collapse, and did not bend.

4.2.2. During Test Behavior and Crack Patterns

From the results, it can be noticed that relatively large deflection for the concrete corbel is associated with the lower specimen strength, which is due to the fact that the C30 specimen resists much more stress, for which it deflects more. The first visible shear crack was delayed to be viewed at C30 compared to C15 by 48%, while the flexural crack was viewed after a difference of 53.3%, as listed in Table 5.

Specimen C15 under monotonic load cracked initially, with a single major crack appearing at 7 kN, which was viewed approximately at the corbel face from the column side, while the second crack formed at 16kN and it was a diagonal shear crack (45 degrees inclined). By the continuity of applying the load, the second crack started to widen and propagate, leading to failure at a load of 47.5 kN. Increasing the application of load led to form other new diagonal cracks rapidly until failure. The collapse of this specimen occurred when a large crack initiated at the intersection point of the corbel and column face, going to the point of applied load as shown in Fig. 11. The results in terms of total applied load versus net deflection are shown in Fig.13.

Table 5. Ultimate load, the first visible crack in shear and flexure, and deflection for the tested models

Model symbol	Load (kN)			Displacement (mm)
	1st visible flexural crack	1st visible shear crack	Pu	
C15	7	16	47.5	2.15
C20	11	20	53	2.68
C25	11	23	65	2.83
C30	15	31	88	3.36
a/d=1	52	46	124.8	4.39
a/d=0.75	64	68	200	3
a/d=0.5	115	57	300	3.13
a/d=0.35	Not observed	72	358.7	1.92

After testing specimen C20, it was concluded that flexural cracks were observed first after reaching the applied load of 11 kN, then a few diagonal cracks were observed. The flexural cracks, when applying more load, grew upward and got wider. At the same time, the diagonal crack propagated towards the supporting point as shown in Fig.14. The ultimate load of this model was 53 kN, and when comparing with the previous model, the corbel gained 11.5% of ultimate strength after increasing the concrete compressive strength from 12.5-17 MPa.

Fig. 13. Crack Pattern for C15 corbel

Fig. 14. Crack Pattern of C20 model

Similar failure patterns were observed from the model C25. Flexural cracks were observed first, at approximately 11 kN, and then a few diagonal cracks were observed. After applying more load, the flexural cracks extended upward and became wider. When more axial load was applied to the corbel, diagonal cracks propagated towards the supporting point as shown in Fig.15. The first major diagonal crack appeared at 23 kN, and the failure load reached 65 kN. When comparing with the other previous models, it can be concluded that the compressive strength has a significant influence on the corbel failure load. The crack pattern of the C30 corbel specimen is shown in Fig.16. Shear cracks occurred at loads higher than those of corbel specimens C.15 and C25, which were observed at 31 kN of applied load. The corbel finally collapsed at 88 kN of monotonically increasing compression load, with a development in corbel strength reaching 85% when compared with specimen C15.

Fig. 15. Model C25 after failure

Fig. 16. Crack Pattern of the specimen C30

4.2.3. Initial Stiffness

The initial stiffness is the slope of load-deflection curves at the initial stage of loading within the elastic range. It represents the magnitude of resistance of the model to displacement in the earlier stages of loading, concrete efficiency, steel reinforcement amount and distribution, and the bond between steel and concrete. Initial stiffness was calculated as the slope between the origin and first cracking load, which is listed in Table 6; it can be noticed that corbels' initial stiffness increases after increasing concrete compressive strength by 108% when comparing C15 and C30. It represented higher ability to resist cracks and deflections in the earlier stages. For the models which examining the a/d ratio, a significant enhancement in the initial stiffness occurs after minimizing the a/d ratio due to the arch action activation and generating the strut within corbels. The initial stiffness increases by 64%, 168%, and 412.3% when changing the a/d ratio from 1 to 0.75,0.5 and 0.35, respectively. As a conclusion, the higher concrete compressive strength gives the model higher initial stiffness to resist deformations, and a higher a/d ratio enlarges the arch action and forms the strut of deep beams, which raises corbel strength and initial stiffness.

Table 6. Initial stiffness variation due to strength and geometry (kN/mm)

Compressive strength specimens		a/d specimens	
Specimen	Stiffness	specimen	Stiffness
C15	12	a/d=1	20.75
C20	20	a/d=0.75	34.04
C25	22	a/d=0.5	55.63
C30	25	a/d=0.35	106.3

4.2.4. Ductility

The ductility shows the ability of a structural member to overcome large deformations after the yielding stage without collapse. It is represented by the ratio between the deflection at collapse and the displacement at yield. The yield displacement could be obtained from load versus deflection curves by indicating a tangent for the linear stage and then drawing another tangent for the plastic zone. The interaction between these two tangents is the point of yield displacement [27]. When a model has higher ductility, it still cracks under loading and still resists as much as possible, but for a specimen with less ductility, its collapse becomes brittle without much resistance. From Table 7, the increase in concrete compressive strength leads to an increase in ductility by 21.05 %, 26.3%, and 47.36% when developing the strength from C15 to C20, C25, and C30, respectively.

Furthermore, casting corbels with lower a/d ratios such as 0.75,0.5 and 0.35 leads to enhanced ductility by 26.08%, 30.43%, and 47.8% compared to a/d=1. It can be concluded that the higher arch action corbels and higher strength lead to far from brittle failure and are safer in constructions due to the ductile behavior, which could be noticed before collapse. To put it another way, this pattern suggests that reducing a/d ratios increases stronger arch action and redistributes loads via compression struts rather than flexural action. Because of the slower fracture propagation, the corbels can experience more post-cracking deformation before failure, which increases their ductility.

Table 7. The impact of studied parameters on ductility

Specimen	Ductility	Specimen	Ductility
C15	1.9	a/d=1	2.3
C20	2.3	a/d=0.75	2.9
C25	2.4	a/d=0.5	3.0
C30	2.8	a/d=0.35	3.4

4.2.5. Toughness

It represents the amount of energy that the member can absorb before failure; the higher toughness, the greater the ability to overcome the load before collapse. Polynomial equations of the sixth degree and an R^2 value (Coefficient of determination) equal to 0.992, then a definite integration was calculated for these polynomials to find the area under the curves. From Table 8, it can be noticed that the increment in concrete compressive strength provides tougher corbels by 75%, 125%, and 256% when increasing the C15 to C20, C25, and C30, respectively. Minimizing the a/d ratio from 1 to 0.75,0.5 and 0.35 enlarges the deep beam effect, which enhances corbels' toughness by 14.75%, 17.48%, and 23.41%, respectively.

Table 8. Magnitude of toughness under different study conditions (KN/mm)

Specimen	Toughness	Specimen	Toughness
C15	41.64	a/d=1	264.8
C20	72.92	a/d=0.75	303.86
C25	93.98	a/d=0.5	311.09
C30	148.5	a/d=0.35	326.8

5. Conclusions

The research conclusions (which are based on the experimental program in which one specimen was examined for each parameter, do not represent statistically verified results; rather, they describe the observed experimental patterns within the parameters of the current investigation) could be summarized by the following points:

- The mode of failure for all specimens ranges between flexural and diagonal-splitting types of failure.
- The same behavior is observed for all specimens from the first group, which discussed the compressive strength effect. The increment in ultimate load is about (11.5%, 37% and 85%) for specimens with compressive strength C20, C25 and C30 MPa, respectively, with respect to the specimen that has C15 MPa.
- Higher toughness was correlated with an increase in concrete compressive strength, with gains of 75%, 125%, and 256% for C20, C25, and C30, respectively, over C15. Similarly, because of the improved deep beam action and more effective load transfer, lowering the a/d ratio from 1.0 to 0.75, 0.5, and 0.35 raised the toughness by 14.75%, 17.48%, and 23.41%, respectively. I.e., increased toughness was linked to higher concrete compressive strength, and toughness was also improved by lowering the a/d ratio because of improved deep beam action, which allowed the corbels to absorb more energy before failing.
- An increment in ductility was observed when maximizing concrete compressive strength by 21.05%, 26.30%, and 47.36% for C20, C25, and C30, respectively, compared with C15. This

trend is explained by the improved capacity of the concrete compression strut, which allowed greater deformation before failure and delayed crushing; similarly, lowering the a/d ratio to 0.75, 30.5, and 47.80%, respectively, resulted from the development of a more effective arch action and delayed the propagation of diagonal cracks.

- Decreasing the horizontal distance relative to the effective depth enhances the arching (compression strut) mechanism, allowing forces to be transferred more directly and efficiently to the column. Therefore, the a/d ratio is the governing parameter controlling the ultimate strength of corbels.
- After cracking, the stiffness dropped due to a transfer of loads toward the reinforcement caused by the creation of diagonal fractures, which lowered the effective concrete area resisting shear. So that, corbels' initial stiffness increases after increasing concrete compressive strength by 108% when comparing C15 to C30. It represents a higher ability to resist cracks and deflections in the earlier stages.
- A significant enhancement in initial stiffness was observed when minimizing the a/d ratio, which is attributed to the activation of arch action and the direct formation of a compressive strut. The initial stiffness increases by 64%, 168%, and 412.3% when changing the a/d ratio from 1 to 0.75,0.5 and 0.35, respectively.
- Specimens with smaller a/d ratios exhibited steeper load–deflection curves and lower deflections, indicating stiffer behavior and an enhancement in the ductile behavior.
- The a/d ratio affects not only the load capacity but also the deformation characteristics and failure mode, which is a critical consideration in structural design.

References

[1] Huang Y, Xia W, Hong Z. Shear behavior of ultra-high performance concrete corbels: Experimental study and modified strut-and-tie model. Eng Struct. 2024;310:118043. https://doi.org/10.1016/j.engstruct.2024.118043

[2] ACI Committee 318. Building code requirements for structural concrete (ACI 318-19) and commentary (ACI 318R-19). Farmington Hills (MI): American Concrete Institute; 2019.

[3] Bobek L, Klusáček L, Svoboda A. Effective strengthening of reinforced concrete corbels using post-tensioning. Eng Struct. 2024;305:117716. https://doi.org/10.1016/j.engstruct.2024.117716

[4] Li SS, Zheng JY, Zhang JH, Li HM, Guo GQ, Chen AJ, et al. Experimental investigation on shear capacity of steel-fiber-reinforced high-strength concrete corbels. Materials (Basel). 2023;16(8):3055. https://doi.org/10.3390/ma16083055

[5] Huang Y, Peng L, Wang H. Finite element analysis of the shear performance of reinforced concrete corbels under different design codes. Buildings. 2024;14(6):1746. https://doi.org/10.3390/buildings14103100

[6] Ali MA, Karim FR. Shear strengthening of RC corbels with carbon fiber reinforced polymer sheets: A critical review. Construction. 2024;4(2):176-185. https://doi.org/10.15282/construction.v4i2.10760

[7] Dawood AA, Kadhum AK, Abdul-Razzak KS. Strength of reinforced concrete corbels - A parametric study. Int J Civ Eng Technol. 2018;9(11):2274-2288.

[8] Megahed K. STM-based symbolic regression for strength prediction of RC deep beams and corbels. Sci Rep. 2024;14(1):25066. https://doi.org/10.1038/s41598-024-74803-9

[9] Attiya MA, Mohamad-Ali AA. Nonlinear analysis of reinforced concrete corbels strengthened with carbon fibre reinforced polymer strips by ANSYS. Kufa J Eng. 2019;10(2):60-75. https://doi.org/10.30572/2018/KJE/100205

[10] Attiya MA. Behaviour of reinforced concrete corbels strengthened with carbon fiber reinforced polymer strips [PhD dissertation]. Basrah: University of Basrah; 2010.

[11] Majeed LA, Kadhum MM, Al-Adili A. Reinforced concrete corbels - State of the art. J Mater Eng Struct. 2015;2(4):180-205.

[12] Reginato L, de Sousa AMD, Santos JVC, El Debs MK. NLFEA of reinforced concrete corbels: Proposed framework, sensibility study, and precision level. Buildings. 2023;13(5):1154. https://doi.org/10.3390/buildings13071874

[13] Attiya MA, Kamonna HH. Performance of steel fiber-reinforced concrete corbels without secondary reinforcement. AIP Conf Proc. 2023;2775:020003. https://doi.org/10.1063/5.0140869

[14] Mohamad-Ali AA, Attiya MA. Experimental behaviour of reinforced concrete corbels strengthened with carbon fibre reinforced polymer strips. Basrah J Eng Sci. 2012;12(1):47-62.

[15] Obin U. Structural design of corbels. Structville; 2020 [accessed 2026]. Available from: https://structville.com/2020/07/structural-design-of-corbels.html

[16] AlShamaa KQ, Al-Khafaji MF. Experimental study of behaviour of reactive powder concrete strengthening by NSM-CFRP corbels. Civ Eng J. 2018;4(5):1052-1064. https://doi.org/10.28991/cej-0309150
[17] Sadoon EK, Radhi AS. Shear strength capacity of reinforced concrete corbels. Tikrit J Eng Sci. 2024;31(4):112-124. https://doi.org/10.25130/tjes.31.4.7
[18] Huang H, Xue C, Wang Z. Experimental and numerical simulation study on shear performance of RC corbel under synergistic change in inclination angle. Structures. 2025;71:107890. https://doi.org/10.3390/buildings15173098
[19] Hameed AH, Kadhum MM. Shear resistance of fibrous reinforced concrete corbels - A critical review. J Eng Sustain Dev. 2022;26(1):66-78. https://doi.org/10.15282/construction.v2i1.7608
[20] Lei H, Wu F, Gao L, Yan J, Huang H. Experimental study and kinematics-based approach for shear strength assessment of RC corbels with variously inclined reinforcement. Eng Struct. 2025;341:120830. https://doi.org/10.1016/j.engstruct.2025.120830
[21] Traad HZ, Elesnawi HH. Enhancement of reinforcement concrete corbels using pre-stressing technique. J Al-Azhar Univ Eng Sect. 2026;21(78):115-128.
[22] Central Organization for Standardization and Quality Control. Iraqi Standard Specification No. 5: Portland cement. Baghdad: COSQC; 1984. p. 1-8.
[23] Central Agency for Standardization and Quality Control. Iraqi standard specifications for aggregate sizes (IQS No. 45). Baghdad: CASQC; 1984.
[24] Makki OM, Al-Mutairee HMK. Continuous deep beams behavior under static loads: A review study. IOP Conf Ser Earth Environ Sci. 2022;1002:012015. https://doi.org/10.1088/1755-1315/961/1/012034
[25] Zhang N, Tan KH. Direct strut-and-tie model for single span and continuous deep beams. Eng Struct. 2007;29(11):2987-3001. https://doi.org/10.1016/j.engstruct.2007.02.004
[26] Altaan S. Strut and tie model for the analysis of fibre reinforced concrete deep beams [thesis]. Mosul: University of Mosul; 2018.
[27] Sharbatdar MK, Ghods A, Sennah K. Enhancing flexural behavior and ductility of fixed-end RC beams using high-performance fiber-reinforced cementitious composites. Int J Concr Struct Mater. 2025;19(1):1-27. https://doi.org/10.1038/s41598-025-25190-2